Published in final edited form as:
Mol Cancer Ther. 2014 May ; 13(5): 1323–1333. doi:10.1158/1535-7163.MCT-13-0904.

The G-protein Coupled Receptor GALR2 Promotes Angiogenesis in Head and Neck Cancer

Rajat Banerjee[1,*], **Elizabeth A. Van Tubergen**[1,*], **Christina S. Scanlon**[1], **Robert Vander Broek**[1], **Joel P. Lints**[1], **Min Liu**[1], **Nickole Russo**[1], **Ronald C. Inglehart**[1], **Yugang Wang**[1], **Peter J. Polverini**[1], **Keith L. Kirkwood**[2], and **Nisha J. D'Silva**[1,3]

[1]Department of Periodontics and Oral Medicine, University of Michigan School of Dentistry, Ann Arbor, Michigan

[2]Department of Craniofacial Biology, The Medical University of South Carolina, Ann Arbor, Michigan

[3]Department of Pathology; University of Michigan Medical School, Ann Arbor, Michigan

Abstract

Squamous cell carcinoma of the head and neck (SCCHN) is an aggressive disease with poor patient survival. Galanin Receptor 2 (GALR2) is a G-protein coupled receptor (GPCR) that induces aggressive tumor growth in SCCHN. The objective of this study was to investigate the mechanism by which GALR2 promotes angiogenesis, a critical oncogenic phenotype required for tumor growth. The impact of GALR2 expression on secretion of pro-angiogenic cytokines in multiple SCCHN cell lines was investigated by ELISA and *in-vitro* angiogenesis assays. Chemical inhibitor and genetic knockdown strategies were used to understand the key regulators. The *in-vivo* impact of GALR2 on angiogenesis was investigated in mouse xenograft, chick chorioallantoic membrane (CAM) and the clinically-relevant mouse orthotopic floor-of-mouth models. GALR2 induced angiogenesis via p38-MAPK-mediated secretion of pro-angiogenic cytokines, VEGF and IL-6. Moreover, GALR2 activated small-GTP-protein, RAP1B, thereby inducing p38-mediated inactivation of tristetraprolin (TTP), which functions to destabilize cytokine transcripts. This resulted in enhanced secretion of pro-angiogenic cytokines and angiogenesis *in-vitro* and *in-vivo*. In SCCHN cells overexpressing GALR2, inactivation of TTP increased secretion of IL-6 and VEGF, whereas inhibition of p38 activated TTP and decreased cytokine secretion.

Here we report that GALR2 stimulates tumor angiogenesis in SCCHN via p38-mediated inhibition of TTP with resultant enhanced cytokine secretion. Given that p38 inhibitors are in clinical use for inflammatory disorders, GALR2/p38-mediated cytokine secretion may be an excellent target for new adjuvant therapy in SCCHN.

Correspondence and reprint requests should be addressed to: Nisha J. D'Silva, 1011 N. University Ave, Rm 5217, Dept of Periodontics and Oral Medicine, University of Michigan, School of Dentistry, Ann Arbor, MI 48109-1078, Phone: (734) 764-1543, Fax: (734) 764-2469, njdsilva@umich.edu.
*Contributed equally to this study.

CONFLICT OF INTEREST: All authors in this manuscript declare no conflict of interest.

Keywords

GALR2; RAP1B; p38; tristetraprolin (TTP); cytokines; VEGF; IL-6

INTRODUCTION

Each year nearly 600,000 individuals are diagnosed with SCCHN, which is the sixth most common cancer globally (1). Despite treatment, almost half of the patients die-of-disease within five years of diagnosis (1). Elucidating the mechanisms that support tumor progression will facilitate the development of mechanism-based treatment strategies. Angiogenesis has a critical role in tumor progression (2–3). For example, the vasculature provides nutrients and oxygen to the tumor as well as an avenue to eliminate metabolic waste and CO_2 (3). Continuous neovascularization facilitates tumor growth and spread (2).

In SCCHN, angiogenesis is activated by cytokines including interleukin-6 (IL-6) and vascular endothelial growth factor (VEGF) (4–5). IL-6 is a biomarker for poor disease-specific-survival (6) and high VEGF correlates with reduced time-to-disease recurrence (7). Inhibitors to IL-6 and VEGF were developed to target the vasculature of multiple solid tumors (8). However, though VEGF inhibitors are used as an adjuvant to chemotherapy in colorectal cancer, the drug does not prevent disease recurrence (9). In breast cancer, VEGF inhibitors only marginally improved survival, possibly due to redundancy in function between cytokines. In fact, approval of VEGF inhibitors for treatment of breast cancer was recently revoked(10).

IL-6 and VEGF are regulated post-transcriptionally to enable rapid modulation of protein expression (11). mRNA is actively degraded or stabilized by RNA-binding proteins (RNA-BPs) that bind AU-rich elements in the 3′untranslated region. TTP is an RNA-BP that promotes decay of transcripts of pro-angiogenic factors including IL-6, VEGF and IL-8 in cancer and inflammatory cells (6, 12–13). Downregulation of TTP in SCCHN leads to transcript stability and enhances secretion of IL-6 and VEGF (6) but its role in tumor angiogenesis has not been investigated.

p38-MAPK is a critical signaling molecule that activates cytokines. In SCCHN and multiple myeloma, p38 is constitutively active and promotes tumor growth, survival and invasion by modulating secretion of multiple cytokines and pro-inflammatory mediators (14) but its role in angiogenesis is unexplored.

Human GAL, a 30 amino acid neuropeptide, promotes pain, nociception, and cell survival in the central and peripheral nervous systems (15). GAL is secreted by non-neuronal cells, such as keratinocytes, including malignant keratinocytes (16–17). GAL induces its biological effects via three GPCRs, GALR1, GALR2 and GALR3 (18). Only GALR1 and GALR2 have been linked to tumorigenesis in non-neuronal cells (19). GALR1 is frequently silenced in SCCHN and has a tumor suppressive effect (17, 20) whereas GALR2 promotes tumor proliferation and survival (16). GALR2 is unchanged or overexpressed in SCCHN compared to normal human keratinocytes (16, 21). Even without a change in expression, GAL-induced GALR2 signaling may be amplified by concurrent downregulation of GALR1 (21).

A previous study showed that GALR2 induces angiogenesis during wound healing (22) but its role in tumor angiogenesis was unknown. Using small cell lung cancer cell lines, Yamamoto et al (23) recently showed that GAL stimulates angiogenesis but the signaling cascade was uncharacterized. In the present study, we show that GAL induces angiogenesis via GALR2-induced, RAP1B-p38-mediated IL-6 and VEGF secretion. RAP1B, a ras-like protein, shuttles between inactive GDP- and active GTP-bound forms. Given the importance of pro-angiogenic cytokines such as IL-6 and VEGF in tumor progression, inhibition of secretion of these factors by targeting a common upstream regulator may be a promising strategy to suppress angiogenesis and tumor progression.

MATERIALS AND METHODS

Cell culture

SCCHN cell lines (T. Carey, University of Michigan) were cultured as described and validated by genotyping at the Sequencing Core (University of Michigan) before and at the end of the study (24–25). An immortalized human microvascular endothelial cell line HMEC-1 (Center for Disease Control) was used for sprouting assays. HMEC-1 cells were maintained in MCDB-131 media (Gibco) supplemented with 10% FBS, 1% glutamine, 1% penicillin/streptomycin and 1 ng/ml epidermal growth factor.

Conditioned medium (CM)

CM was collected as described (6). Briefly, SCCHN cells at ~60–70% confluence were cultured in DMEM without supplements. After 24h the medium was centrifuged and the supernatant (CM) was collected and concentrated using 3kDa centrifugal filters (Millipore).

Transfection and knockdown

For transient knockdown of p38, ON-target-SMART-pool siRNA (Dharmacon) was used. To downregulate TTP and IL-6, four siRNAs were screened for each target; siRNAs yielding optimal, sustained knockdown were used (26). Transfections were performed as described (6). UM-SCC-1 and UM-SCC-81B cells were stably transfected with pcDNA3.1-GALR2 or pcDNA3.1 as described (16).

For stable knockdown of TTP, UM-SCC-1 and -81B cells were transduced with short hairpin RNA shTTP and shControl (scramble) in lentiviral particles (Open Biosystems) (26). For stable knockdown of VEGF in UM-SCC-1-GALR2 cells, cells were transduced with shVEGF (Open Biosystems). Stable cell lines were selected in 10μg/ml puromycin (Sigma).

Western blot analysis

Cell lysates were electrophoresed (6) and incubated with primary antibodies (concentration 1:1000 unless otherwise indicated): phospho-p38 (p-p38), total p38 (p38), actin, RAP1B (Cell Signaling), TTP (SantaCruz), p-Serine (Abcam), IL-6 (R&D Systems), GALR2 (Alpha Diagnostics) and GAPDH (Millipore/Upstate). HRP-conjugated secondary antibodies (Jackson Immuno-Research) were visualized by SuperSignal Substrate (Pierce).

Immunoprecipitation

TTP was immunoprecipitated with TTP antibody (SantaCruz) crosslinked to Amino-Link Plus Coupling Resin (Pierce) supplemented with protease (Roche) and phosphatase (Sigma) inhibitors.

Enzyme linked immunosorbent assay (ELISA)

IL-6 and VEGF-A were quantified by non-competitive ELISA (R&D Systems).

Endothelial tube formation (sprouting) assay

Growth factor-depleted Matrigel (BD Biosciences) was coated on a chamber slide (BD Biosciences) as described (27). CM was normalized to cell number and volume, and resuspended in MCDB-131 media containing 3% FBS. HMEC-1 cells (4×10^4) were seeded in triplicate in 150μl of CM from cells transfected with non-target (NT), sip38, siTTP or siIL-6. VEGF (1ng/ml) was used as a positive control in initial experiments (not shown). DMEM served as a negative control. Digital images of endothelial tubes were taken after 24h (5 random fields/well). Endothelial tubes were counted in each field to determine tube number. Tube length was determined with ImageJ software using arbitrary units.

GALR2 studies

For activation studies, UM-SCC-1-GALR2 and -pcDNA cells were serum-starved for 4h and treated with 10 nM GAL (Sigma) as described (16). For inhibition studies, UM-SCC-1-GALR2 cells were incubated with GALR2-specific antagonist M871 (Tocris Bioscience, 100nM) with DMSO as control.

Inhibition of p38-MAPK

Cells were serum-starved for 4h and incubated with 10μM of SB203580 (Promega) for 1h.

In-vivo studies and immunohistochemistry

All *in-vivo* studies were done according to University of Michigan University Committee on Use and Care of Animals (UCUCA) approved protocols. UM-SCC-1-GALR2 and -pcDNA (1×10^6) were injected subcutaneously (n=10, 5 in each group) in athymic mice (Ncr nu/nu strain, NCI) for tumor growth as reported (16). Angiogenesis of the tumor was quantified by measuring vascular density (redness) normalized to surface area with Image-J software. For the clinically relevant floor-of-mouth xenograft model of SCCHN, UM-SCC-81B-shTTP and control cells (1×10^6) were implanted submucosally in the floor-of-mouth of athymic mice (28). Immunohistochemistry was performed on tissue sections for pancytokeratin (Millipore) (29) and Factor-VIII (DAKO).

Chicken CAM

Cells were seeded on the CAM, an *in-vivo* model of angiogenesis in SCCHN (30). AngioTool (https://ccrod.cancer.gov/confluence/display/ROB2/Home) was used to quantify the vasculature.

Data analysis

Statistical analysis was performed using a Student's *t*-test. A p-value of < 0.05 was considered to be statistically significant. Densitometry was performed using ImageJ software.

RESULTS

GALR2 induces angiogenesis

Previously we showed that overexpression of GALR2 in multiple SCCHN cell lines induces proliferation and survival *in-vitro* and aggressive tumors in the mouse (16). In the present study, we show that tumors generated from UM-SCC-1-GALR2 cells are more vascular than control tumors in the mouse. As shown in Fig. 1A, the UM-SCC-1-GALR2 tumors are more reddish-brown than control tumors, compatible with more vascularity (left panel and graph). Increased vascularity was verified by immunostaining with Factor-VIII on tissue sections. Blood vessels, which stained positively for Factor-VIII increased by two-fold in UM-SCC-1-GALR2 compared to control tumors (Fig. 1A, middle-right and right panels, respectively). The microscopic appearance and cytokeratin immunoreactivity of the tumors was consistent with SCCHN. IgG controls were appropriately negative (not shown).

To independently verify the angiogenic potential of GALR2 in SCCHN, we used the CAM model (30). UM-SCC-1-GALR2 cells seeded on the CAM induced larger, more angiogenic tumors than control UM-SCC-1-pcDNA cells (Fig. 1B, left panel), consistent with mouse studies (Fig. 1A) (16). Around the tumor, the vascularity (Fig. 1B, middle-left panel), as quantified by branching points (white arrowheads) and length of blood vessels (white arrows) was higher in UM-SCC-1-GALR2 compared to control tumors (Fig. 1B, middle-right graphs). Corresponding tissue sections of the CAM showed more vasculature in UM-SCC-1-GALR2 tumors than controls (Fig. 1B, right panel). Similar results were observed with UM-SCC-81B-GALR2 an independent SCCHN cell stably overexpressing GALR2 (Supplemental Fig. S1A and B). Consistent with a role for GALR2 in angiogenesis, the GALR2 specific inhibitor M871 reduced vascularity *in-vivo* (Supplemental Fig. S2). To verify whether the enhanced vascularity is mediated by cytokines secreted from tumor cells, *in-vitro* sprouting assays were performed. Endothelial cells (HMEC-1) were incubated with conditioned media (CM) from UM-SCC-1-GALR2 or control cells. The number and length of tubes (arrows) were increased in HMEC-1 cells that were incubated with CM from UM-SCC-1-GALR2 cells (Fig. 1C, left-middle panel and graphs). GALR2 overexpression was confirmed by immunoblot analysis (Fig. 1C, left panel, also for UM-SCC-81B-GALR2 in Fig. S1B, bottom panel). The *in-vitro* and *in-vivo* studies support that GALR2 induces angiogenesis, a hallmark of tumor progression.

GALR2 stimulates cytokine secretion and angiogenesis via RAP1B, p38

Given the emerging importance of p38 in angiogenesis (3), the role of GALR2 in p38 stimulation was investigated. To do so, endogenous GALR2 was downregulated in UM-SCC-1 cells (Supplemental Fig. S3). Loss of GALR2 expression by two siRNAs (siGALR2–7 & siGALR2–10) resulted in downregulation of phospho-p38 (Supplemental Fig. S3), which verifies that p38 is induced by GALR2. In complementary gain-of-function

experiments, endogenous p38 activation was observed in UM-SCC-1-GALR2 cells compared to controls (Fig. 2A&2B left panels also in UM-SCC-81B-GALR2 cells in Supplemental Fig. S1B, top panels). Moreover phosphorylation of p38 increased more rapidly in UM-SCC-1-GALR2 cells stimulated with 10nM GAL compared to control pcDNA cells (Fig. 2A left panel).

RAP1B, ras-like protein, is a critical mediator of signaling in SCCHN (16). To investigate the role of RAP1B in GAL-induced p38 activation (Fig. 2A right panel), RAP1B was downregulated with siRAP1B in UM-SCC-1-GALR2 cells, which were seeded at equal density and stimulated with 10nM GAL. GAL-induced p38 activation (Fig. 2A-right panel, lane 2 compared to 1) was inhibited by siRAP1B (Fig. 2A-right panel, lanes 3 and 4).

To investigate if GALR2 induces angiogenesis via p38, initial studies focused on whether pro-angiogenic cytokine secretion is induced by GALR2 via p38. UM-SCC-1-GALR2 cells secrete almost two-fold more VEGF and IL-6 than control cells (Fig. 2B middle and right panels respectively), correlating with increased phospho-p38. Importantly, downregulation of p38 in UM-SCC-1-GALR2 cells reduced secretion of VEGF and IL-6 (Fig. 2C) thereby establishing that GALR2 induces cytokine secretion via p38. Similar results were obtained with UM-SCC-81B-GALR2 cells, another SCCHN cell line (Supplemental Fig. S4). In corresponding endothelial tube-formation assays, downregulation of p38 significantly reduced tube number and length (Fig. 2D). Taken together, GALR2 induces cytokine secretion and endothelial tube formation via RAP1B-mediated p38 activation.

GALR2 promotes angiogenesis via p38-TTP mediated cytokine secretion

We previously showed that p38 phosphorylates TTP, which destabilizes transcripts including matrix metalloproteinases and IL-6 (26). Since GALR2 induces p38 (Fig. 2B), we investigated the extent to which GALR2 induces VEGF and IL-6 via p38-mediated phosphorylation of TTP, using biochemical and RNAi approaches outlined in Fig. 3A (left panel). To determine whether GALR2 induces p-TTP via p38, UM-SCC-1-GALR2 cells were stimulated with 10nM GAL in the presence or absence of p38 inhibitor SB203580 (Fig. 3 right panel). TTP was immunoprecipitated and immunoblotted with phospho-serine and TTP antibodies. GAL induced phosphorylation of TTP by more than 50% (Fig. 3A-right panel, lane 4 compared to 3), which was abrogated in the presence of SB203580 (Fig. 3A-right panel, lanes 5 and 6), a potent inhibitor of p38-α- and -β catalytic subunits (31).

Phosphorylation of TTP inhibits its ability to target transcripts for degradation thereby enhancing cytokine secretion (26). Therefore, we investigated if GALR2 induces pro-angiogenic cytokines via TTP (Fig. 3B). UM-SCC-1-GALR2 cells transfected with NT-siRNA or siTTP were incubated with SB203580 or vehicle. Compared to baseline, the p38 inhibitor, which increases functional TTP, reduced expression and secretion of VEGF in cell lysate (Fig. 3B left panel, lanes 1 and 2) and CM (middle graph, bars 1 and 2), respectively. In contrast, siTTP enhanced VEGF expression (Fig. 3B left panel, lanes 1 and 3) and secretion (middle graph, bars 1 and 3). As expected, siTTP inhibited the effect of SB203580; there is no significant difference between VEGF expression (left panel, lanes 1 and 4) and secretion (middle graph, bars 1 and 4) compared to baseline. Similar results were observed for IL-6 but the impact of siTTP was more profound on IL-6 secretion (Fig. 3B, right graph)

than cellular expression (Fig. 3B-left panel, immunoblot for IL-6), possibly due to rapid secretion of IL-6 (32). Knockdown of TTP was verified (Fig. 3B left panel).

Given that GALR2 promotes angiogenesis (Fig. 1) and induces secretion of multiple cytokines, (Fig. 2), we verified that GALR2 induces angiogenesis via VEGF and IL-6. VEGF was stably downregulated by shRNA to VEGF and control in UM-SCC-1-GALR2 cells (Fig. 3C, left panel). Endothelial sprouting was quantified after incubation with CM collected from shVEGF and shControl cells (Fig. 3C, middle-left panel). Tube length and number were significantly reduced by 50% in the UM-SCC-1-GALR2-shVEGF compared to UM-SCC-1-GALR2-shControl (Fig. 3C, graphs). Loss-of-function experiments with siIL-6 in UM-SCC-1-GALR2 had a similar effect and also decreased endothelial sprouting (Fig. 3D).

Suppression of TTP promotes angiogenesis

Since GALR2-mediated phosphorylation of TTP induces pro-angiogenic cytokines (Fig. 3B, 3C), TTP's role in angiogenesis was investigated. CM collected from UM-SCC-1 cells transfected with siTTP or NT-siRNA were used in sprouting assays. Downregulation of TTP was verified (Fig. 4A, left panel). Endothelial tube-formation and length were increased 2-fold by siTTP compared to NT-siRNA (Fig. 4A, middle-left panel and right graphs). To further investigate the effect of TTP knockdown on IL-6, IL-6 was downregulated in UM-SCC-1-shTTP cells. Within 36h, downregulation of IL-6 (Fig. 4B, left panel) inhibited endothelial tube-formation (Fig. 4B middle-left panel and right graphs). The impact of TTP suppression on tumor angiogenesis *in-vivo* was investigated on the CAM. A significant increase in vascularity (white arrows) and branching points (white arrowheads) was observed with UM-SCC-1-shTTP compared to control cells, (Fig. 4C left panels). Corresponding CAM tissue sections showed greater vascularity in UM-SCC-1-shTTP than control tumors (Fig. 4C middle-right and right panels respectively).

Downregulation of TTP induces angiogenesis *in-vivo*

From our previous study (28), human UM-SCC-81B cells induce tumor growth in the floor-of-mouth murine model and recapitulate human SCCHN progression. Therefore, this cell line was used for mouse studies. Initially we verified that siTTP in UM-SCC-81B induced angiogenesis *in-vitro*. As observed with UM-SCC-1, siTTP in UM-SCC-81B increased endothelial tube number and length by more than 2-fold and 1.5-fold, respectively, compared to control cells (Fig. 5A middle-left panel and graphs). TTP knockdown was verified (Fig. 5A left panel). Knockdown of IL-6 in stable UM-SCC-81B-shTTP cells significantly reduced endothelial tube number and length (Fig. 5B).

Using the murine floor-of-mouth xenograft model (17, 33), we investigated the impact of TTP-mediated angiogenesis on tumor growth in a location commonly involved by human SCCHN. UM-SCC-81B-shTTP and control cells were implanted submucosally in the floor-of- mouth of nude mice (n=6, 3 control and 3 test group). As shown *in-vitro* (Fig. 5A), downregulation of TTP in UM-SCC-81B induced angiogenesis and tumor growth *in-vivo* (Fig. 5C, left, representative mice with tumor, compared to control). Mice injected with control cells did not have clinically detectable tumors in the same time frame (Fig. 5C, left

panel). Histologically, the tumors exhibited SCCHN morphology (Fig. 5C, middle panel). The epithelial origin of the tumors was verified by immunostaining for pancytokeratin. One of the control mice grew a tumor that was observed on tissue sections although it was not clinically detectable. Immunostaining facilitated visualization and quantification of blood vessels. The average number of blood vessels/10 high-power-fields was significantly higher in the tumors generated from UM-SCC-81B-shTTP than control tumors (Fig. 5C, right panel). Together the *in-vitro* and *in-vivo* data support that downregulation of TTP promotes angiogenesis via release of pro-angiogenic cytokines.

DISCUSSION

In the present study, we demonstrated that GALR2, a pro-survival GPCR, induces angiogenesis via p38-mediated phosphorylation of TTP and enhanced secretion of VEGF and IL-6. Importantly, the pro-angiogenic phenotype of GALR2 was observed *in-vivo* in murine tumor xenografts and in the CAM model. This is the first study establishing the role of GALR2 in tumor-associated angiogenesis, a critical phenotype and treatment target in cancer progression.

Angiogenesis, one of the six hallmarks of cancer (3), facilitates tumor progression by supplying oxygen and nutrients. Although GAL expression is correlated with increased microvessel density in inflammatory tissue in the dermis and stimulates angiogenesis in small cell lung cancer cell lines, the role of GALR2 in tumor angiogenesis is unknown (22–23). In this study, we show that in SCCHN, GALR2 enhances secretion of pro-angiogenic cytokines, IL-6 and VEGF, and induces angiogenesis via RAP1B-p38-mediated inactivation of TTP. SCCHN secretes IL-6 and VEGF, which has been linked with poor patient survival (6, 34) (7). Tumor-derived IL-6 and VEGF promote angiogenesis via paracrine signaling to endothelial cells (35). Knockout of a single VEGF allele in mice is embryonic lethal suggesting that VEGF is critical for maintenance and development of the vasculature (36). To maintain proper vasculature in healthy tissue, there is a delicate balance between angiogenic and anti-angiogenic factors; an imbalance in favor of pro-angiogenic factors promotes tumor growth and spread (37). Therefore, angiogenesis is a promising treatment target to inhibit tumor growth.

Since angiogenesis is critical for tumor progression, drugs targeting either IL-6 or VEGF were developed, but treatment with an individual inhibitor showed marginal improvement in patient survival (38). In phase II clinical trials in breast cancer patients, concurrent monoclonal VEGF antibody and chemotherapy compared to chemotherapy alone showed little increase in disease-free survival (39). Surprisingly, in mouse studies, short-term treatment with VEGF antibody lead to more aggressive tumors (40). The possibility of redundancy in function of pro-angiogenic cytokines suggests that it would be beneficial to identify proteins that target multiple cytokines concurrently. In the present study, we show that GALR2 promotes secretion of IL-6 and VEGF and inhibition of GALR2 using a small molecule, lead to inhibition of angiogenesis.

Previously we showed that GALR2 induces other oncogenic phenotypes including growth and cell survival via the ERK and Akt pathways, respectively (16). In this study, we show

that GALR2 promotes cytokine secretion and angiogenesis via GALR2-RAP1-p38MAPK-mediated inactivation of TTP. Induction of multiple oncogenic phenotypes by GALR2 maybe via induction of multiple signaling pathways. For example, in lung cancer cells, GALR2 induces diverse signaling via three different G-proteins, Gi, Gq and G12 (41). Since GALR2 also induces tumor growth and cell survival in SCCHN (16), targeting GALR2 may inhibit angiogenesis and other oncogenic phenotypes.

p38 is critical for induction of inflammatory pathways (42) and is constitutively active in SCCHN (42). p38-MAPK is stimulated by interleukin-1β (IL-1β), in different cell types (26, 43). Previously we showed that IL1β-induced p38 promotes transcript stability and secretion of IL-6, PGE_2 and VEGF (5). While macrophages, tumor cells and cells in the tumor microenvironment secrete IL-1β to stimulate p38, tumor-derived GAL may also induce p38. Additionally, exposure to sodium pyruvate phorbol-12-mysritate-13-acetate, a potent tumor promoter, induces pro-inflammatory secretion via p38 activation (42). p38 inhibitors were used with some success in the treatment of inflammatory diseases to limit adverse sequelae and may be a potential adjuvant therapy in SCCHN. p38 inhibitors reduced tumor-size in multiple myeloma (44), which may be attributed to reduced IL-6 secretion (45). In our study we successfully used the p38 inhibitor SB203580 to reduce cytokine secretion.

In SCCHN, we showed recently that p38-MAPK phosphorylates (inactivates) TTP thereby stabilizing cytokine transcripts, secretion and invasion (26). TTP binds to the 3′UTR of VEGF, IL-6 and PGE_2 transcripts to promote degradation (26). Given the conservation of this region in multiple cytokines, it is likely that other VEGF isoforms are upregulated by the GALR2-induced cascade. VEGF-C promotes lymphangiogenesis thereby contributing to metastasis to lymph nodes (46–47) which is an important issue for oral cancer spread. VEGF and IL-6 are also transcriptionally regulated by NF-kB, AP-1 and NF-IL6 (48). There is also convincing evidence that VEGF is regulated by mTOR and HIF (49). The present study establishes an additional key upstream regulatory pathway, GALR2-RAP1-p38, in cytokine secretion.

RAP1 is a small GTP-binding protein that is emerging as a significant signaling molecule in SCCHN. In previous studies we showed that RAP1 mediates ERK and Akt activation (16). In the present study, we showed that RAP1 induces p38. While RAP1 may induce multiple signaling cascades, the diversity may also be due to variation in RAP1 isoforms (24). We are currently investigating this possibility.

We and others have shown that GALR2 is expressed in multiple SCC cell lines, including UM-SCC-(1, -22B, and -11A) (17, 21, 50). Our current and previous studies established GALR2 expression via both RT-PCR and immunoblot (16, 28). A study performed solely in UM-SCC-1 detected GALR2 transcript (50) but subsequent reports from the same group stated that GALR2 is not expressed in SCCHN (51–52). The anti-proliferative and anti-apoptotic roles for GALR2 shown in these studies may be due to the high concentrations of GAL (1μM), which do not replicate *in-vivo* conditions where GAL is present at nanomolar or lower concentrations (53). For this and previous studies (16), we used physiologic doses of GAL and consistently show that GALR2 promotes proliferation, cell survival and

angiogenesis. Moreover our in-vitro and *in-vivo* studies were performed in multiple validated SCCHN cell lines, using complementary overexpression and knockdown approaches. Recently, Misawa et al, (54) showed that GALR2 is silenced in almost one-third of SCC. Taken together with our findings, these studies support that GALR2 has a significant role in tumor progression in ~70% of SCCHN.

In summary, our work establishes the importance of GAL/GALR2 in tumor progression via RAP1B-p38-mediated angiogenesis. Since GAL, the ligand for GALR2, is a neuropeptide, our work elucidates an important regulatory mechanism for angiogenesis potentially under the influence of the neuronal system. Given the role of GALR2 in multiple additional oncogenic phenotypes including growth, survival and angiogenesis, the GALR2-induced signaling cascade may be an important treatment target in SCCHN.

Supplementary Material

Refer to Web version on PubMed Central for supplementary material.

Acknowledgments

We thank John Westman for assistance in preparing histological specimens and Tarek Metwally for CAM data analysis.

Financial support: This work was supported by National Institute of Dental and Craniofacial Research grants DE018512 and DE019513 to N. J. D'Silva; F30 DEO21293 to C. S. Scanlon and 5F32 DE213052 to E. A. Van Tubergen.

References

1. Leemans CR, Braakhuis BJ, Brakenhoff RH. The molecular biology of head and neck cancer. Nat Rev Cancer. 2011; 11:9–22. [PubMed: 21160525]
2. Hanahan D, Folkman J. Patterns and emerging mechanisms of the angiogenic switch during tumorigenesis. Cell. 1996; 86:353–64. [PubMed: 8756718]
3. Hanahan D, Weinberg RA. Hallmarks of cancer: the next generation. Cell. 2011; 144:646–74. [PubMed: 21376230]
4. Lingen MW. Angiogenesis in the development of head and neck cancer and its inhibition by chemopreventive agents. Crit Rev Oral Biol Med. 1999; 10:153–64. [PubMed: 10759419]
5. Pries R, Nitsch S, Wollenberg B. Role of cytokines in head and neck squamous cell carcinoma. Expert review of anticancer therapy. 2006; 6:1195–203. [PubMed: 17020454]
6. Van Tubergen E, Vander Broek R, Lee J, Wolf G, Carey T, Bradford C, et al. Tristetraprolin regulates interleukin-6, which is correlated with tumor progression in patients with head and neck squamous cell carcinoma. Cancer. 2011
7. Eisma RJ, Spiro JD, Kreutzer DL. Vascular endothelial growth factor expression in head and neck squamous cell carcinoma. American journal of surgery. 1997; 174:513–7. [PubMed: 9374227]
8. Folkman J. Angiogenesis and angiogenesis inhibition: an overview. EXS. 1997; 79:1–8. [PubMed: 9002217]
9. Koukourakis GV, Sotiropoulou-Lontou A. Targeted therapy with bevacizumab (Avastin) for metastatic colorectal cancer. Clinical & translational oncology : official publication of the Federation of Spanish Oncology Societies and of the National Cancer Institute of Mexico. 2011; 13:710–4.
10. D'Agostino RB Sr. Changing end points in breast-cancer drug approval--the Avastin story. The New England journal of medicine. 2011; 365:e2. [PubMed: 21707384]

11. Carballo E, Lai WS, Blackshear PJ. Feedback inhibition of macrophage tumor necrosis factor-alpha production by tristetraprolin. Science. 1998; 281:1001–5. [PubMed: 9703499]
12. Zhao W, Liu M, D'Silva NJ, Kirkwood KL. Tristetraprolin regulates interleukin-6 expression through p38 MAPK-dependent affinity changes with mRNA 3′ untranslated region. Journal of interferon & cytokine research : the official journal of the International Society for Interferon and Cytokine Research. 2011; 31:629–37.
13. Suswam E, Li Y, Zhang X, Gillespie GY, Li X, Shacka JJ, et al. Tristetraprolin down-regulates interleukin-8 and vascular endothelial growth factor in malignant glioma cells. Cancer research. 2008; 68:674–82. [PubMed: 18245466]
14. Alexandrakis MG, Passam FH, Boula A, Christophoridou A, Aloizos G, Roussou P, et al. Relationship between circulating serum soluble interleukin-6 receptor and the angiogenic cytokines basic fibroblast growth factor and vascular endothelial growth factor in multiple myeloma. Annals of hematology. 2003; 82:19–23. [PubMed: 12574959]
15. Xu XJ, Hokfelt T, Wiesenfeld-Hallin Z. Galanin and spinal pain mechanisms: past, present, and future. EXS. 2010; 102:39–50. [PubMed: 21299060]
16. Banerjee R, Henson BS, Russo N, Tsodikov A, D'Silva NJ. Rap1 mediates galanin receptor 2-induced proliferation and survival in squamous cell carcinoma. Cell Signal. 2011; 23:1110–8. [PubMed: 21345369]
17. Henson BS, Neubig RR, Jang I, Ogawa T, Zhang Z, Carey TE, et al. Galanin receptor 1 has anti-proliferative effects in oral squamous cell carcinoma. J Biol Chem. 2005; 280:22564–71. [PubMed: 15767248]
18. Branchek TA, Smith KE, Gerald C, Walker MW. Galanin receptor subtypes. Trends Pharmacol Sci. 2000; 21:109–17. [PubMed: 10689365]
19. Mitsukawa K, Lu X, Bartfai T. Galanin, galanin receptors and drug targets. Cell Mol Life Sci. 2008; 65:1796–805. [PubMed: 18500647]
20. Misawa K, Ueda Y, Kanazawa T, Misawa Y, Jang I, Brenner JC, et al. Epigenetic inactivation of galanin receptor 1 in head and neck cancer. Clin Cancer Res. 2008; 14:7604–13. [PubMed: 19047085]
21. Sugimoto T, Seki N, Shimizu S, Kikkawa N, Tsukada J, Shimada H, et al. The galanin signaling cascade is a candidate pathway regulating oncogenesis in human squamous cell carcinoma. Genes Chromosomes Cancer. 2009; 48:132–42. [PubMed: 18973137]
22. Yamamoto H, Arai T, Ben S, Iguchi K, Hoshino M. Expression of galanin and galanin receptor mRNA in skin during the formation of granulation tissue. Endocrine. 2011; 40:400–7. [PubMed: 21894515]
23. Yamamoto H, Okada R, Iguchi K, Ohno S, Yokogawa T, Nishikawa K, et al. Involvement of plasmin-mediated extracellular activation of progalanin in angiogenesis. Biochem Biophys Res Commun. 2013; 430:999–1004. [PubMed: 23261456]
24. Mitra RS, Zhang Z, Henson BS, Kurnit DM, Carey TE, D'Silva NJ. Rap1A and rap1B ras-family proteins are prominently expressed in the nucleus of squamous carcinomas: nuclear translocation of GTP-bound active form. Oncogene. 2003; 22:6243–56. [PubMed: 13679863]
25. Mitra RS, Goto M, Lee JS, Maldonado D, Taylor JM, Pan Q, et al. Rap1GAP promotes invasion via induction of matrix metalloproteinase 9 secretion, which is associated with poor survival in low N-stage squamous cell carcinoma. Cancer research. 2008; 68:3959–69. [PubMed: 18483282]
26. Van Tubergen EA, Banerjee R, Liu M, Vander Broek R, Light E, Kuo S, et al. Inactivation or Loss of TTP Promotes Invasion in Head and Neck Cancer via Transcript Stabilization and Secretion of MMP9, MMP2, and IL-6. Clin Cancer Res. 2013; 19:1169–79. [PubMed: 23349315]
27. Kumar P, Benedict R, Urzua F, Fischbach C, Mooney D, Polverini P. Combination treatment significantly enhances the efficacy of antitumor therapy by preferentially targeting angiogenesis. Laboratory investigation; a journal of technical methods and pathology. 2005; 85:756–67.
28. Henson B, Li F, Coatney DD, Carey TE, Mitra RS, Kirkwood KL, et al. An orthotopic floor-of-mouth model for locoregional growth and spread of human squamous cell carcinoma. J Oral Pathol Med. 2007; 36:363–70. [PubMed: 17559499]

29. Zhang Z, Mitra RS, Henson BS, Datta NS, McCauley LK, Kumar P, et al. Rap1GAP inhibits tumor growth in oropharyngeal squamous cell carcinoma. The American journal of pathology. 2006; 168:585–96. [PubMed: 16436672]
30. Liu M, Scanlon CS, Banerjee R, Russo N, Inglehart RC, Willis AL, et al. The Histone Methyltransferase EZH2 Mediates Tumor Progression on the Chick Chorioallantoic Membrane Assay, a Novel Model of Head and Neck Squamous Cell Carcinoma. Transl Oncol. 2013; 6:273–81. [PubMed: 23730406]
31. Kumar S, Jiang MS, Adams JL, Lee JC. Pyridinylimidazole compound SB 203580 inhibits the activity but not the activation of p38 mitogen-activated protein kinase. Biochem Biophys Res Commun. 1999; 263:825–31. [PubMed: 10512765]
32. Elner VM, Scales W, Elner SG, Danforth J, Kunkel SL, Strieter RM. Interleukin-6 (IL-6) gene expression and secretion by cytokine-stimulated human retinal pigment epithelial cells. Exp Eye Res. 1992; 54:361–8. [PubMed: 1381679]
33. Wolter KG, Wang SJ, Henson BS, Wang S, Griffith KA, Kumar B, et al. (−)-gossypol inhibits growth and promotes apoptosis of human head and neck squamous cell carcinoma in vivo. Neoplasia. 2006; 8:163–72. [PubMed: 16611409]
34. Duffy SA, Taylor JM, Terrell JE, Islam M, Li Y, Fowler KE, et al. Interleukin-6 predicts recurrence and survival among head and neck cancer patients. Cancer. 2008; 113:750–7. [PubMed: 18536030]
35. Neiva KG, Zhang Z, Miyazawa M, Warner KA, Karl E, Nor JE. Cross talk initiated by endothelial cells enhances migration and inhibits anoikis of squamous cell carcinoma cells through STAT3/Akt/ERK signaling. Neoplasia. 2009; 11:583–93. [PubMed: 19484147]
36. Carmeliet P, Ferreira V, Breier G, Pollefeyt S, Kieckens L, Gertsenstein M, et al. Abnormal blood vessel development and lethality in embryos lacking a single VEGF allele. Nature. 1996; 380:435–9. [PubMed: 8602241]
37. Naumov GN, Akslen LA, Folkman J. Role of angiogenesis in human tumor dormancy: animal models of the angiogenic switch. Cell Cycle. 2006; 5:1779–87. [PubMed: 16931911]
38. Carmeliet P, Jain RK. Molecular mechanisms and clinical applications of angiogenesis. Nature. 2011; 473:298–307. [PubMed: 21593862]
39. Miller KD. E2100: a phase III trial of paclitaxel versus paclitaxel/bevacizumab for metastatic breast cancer. Clinical breast cancer. 2003; 3:421–2. [PubMed: 12636887]
40. Ebos JM, Lee CR, Cruz-Munoz W, Bjarnason GA, Christensen JG, Kerbel RS. Accelerated metastasis after short-term treatment with a potent inhibitor of tumor angiogenesis. Cancer cell. 2009; 15:232–9. [PubMed: 19249681]
41. Wittau N, Grosse R, Kalkbrenner F, Gohla A, Schultz G, Gudermann T. The galanin receptor type 2 initiates multiple signaling pathways in small cell lung cancer cells by coupling to G(q), G(i) and G(12) proteins. Oncogene. 2000; 19:4199–209. [PubMed: 10980593]
42. Riebe C, Pries R, Kemkers A, Wollenberg B. Increased cytokine secretion in head and neck cancer upon p38 mitogen-activated protein kinase activation. International journal of molecular medicine. 2007; 20:883–7. [PubMed: 17982698]
43. Lee JC, Laydon JT, McDonnell PC, Gallagher TF, Kumar S, Green D, et al. A protein kinase involved in the regulation of inflammatory cytokine biosynthesis. Nature. 1994; 372:739–46. [PubMed: 7997261]
44. Medicherla S, Reddy M, Ying J, Navas TA, Li L, Nguyen AN, et al. p38alpha-selective MAP kinase inhibitor reduces tumor growth in mouse xenograft models of multiple myeloma. Anticancer research. 2008; 28:3827–33. [PubMed: 19189670]
45. Ishitsuka K, Hideshima T, Neri P, Vallet S, Shiraishi N, Okawa Y, et al. p38 mitogen-activated protein kinase inhibitor LY2228820 enhances bortezomib-induced cytotoxicity and inhibits osteoclastogenesis in multiple myeloma; therapeutic implications. Br J Haematol. 2008; 141:598–606. [PubMed: 18397345]
46. Patel V, Marsh CA, Dorsam RT, Mikelis CM, Masedunskas A, Amornphimoltham P, et al. Decreased lymphangiogenesis and lymph node metastasis by mTOR inhibition in head and neck cancer. Cancer research. 2011; 71:7103–12. [PubMed: 21975930]

47. POc, Rhys-Evans P, Eccles SA. Expression of vascular endothelial growth factor family members in head and neck squamous cell carcinoma correlates with lymph node metastasis. Cancer. 2001; 92:556–68. [PubMed: 11505400]

48. Ondrey FG, Dong G, Sunwoo J, Chen Z, Wolf JS, Crowl-Bancroft CV, et al. Constitutive activation of transcription factors NF-(kappa)B, AP-1, and NF-IL6 in human head and neck squamous cell carcinoma cell lines that express pro-inflammatory and pro-angiogenic cytokines. Mol Carcinog. 1999; 26:119–29. [PubMed: 10506755]

49. Naruse T, Kawasaki G, Yanamoto S, Mizuno A, Umeda M. Immunohistochemical study of VEGF expression in oral squamous cell carcinomas: correlation with the mTOR-HIF-1alpha pathway. Anticancer research. 2011; 31:4429–37. [PubMed: 22199311]

50. Kanazawa T, Iwashita T, Kommareddi P, Nair T, Misawa K, Misawa Y, et al. Galanin and galanin receptor type 1 suppress proliferation in squamous carcinoma cells: activation of the extracellular signal regulated kinase pathway and induction of cyclin-dependent kinase inhibitors. Oncogene. 2007; 26:5762–71. [PubMed: 17384686]

51. Kanazawa T, Kommareddi PK, Iwashita T, Kumar B, Misawa K, Misawa Y, et al. Galanin receptor subtype 2 suppresses cell proliferation and induces apoptosis in p53 mutant head and neck cancer cells. Clin Cancer Res. 2009; 15:2222–30. [PubMed: 19276245]

52. Uehara T, Kanazawa T, Mizukami H, Uchibori R, Tsukahara T, Urabe M, et al. Novel anti-tumor mechanism of galanin receptor type 2 in head and neck squamous cell carcinoma cells. Cancer Sci. 2013

53. Grenback E, Bjellerup P, Wallerman E, Lundblad L, Anggard A, Ericson K, et al. Galanin in pituitary adenomas. Regul Pept. 2004; 117:127–39. [PubMed: 14700749]

54. Misawa K, Kanazawa T, Misawa Y, Uehara T, Imai A, Takahashi G, et al. Galanin has tumor suppressor activity and is frequently inactivated by aberrant promoter methylation in head and neck cancer. Transl Oncol. 2013; 6:338–46. [PubMed: 23730414]

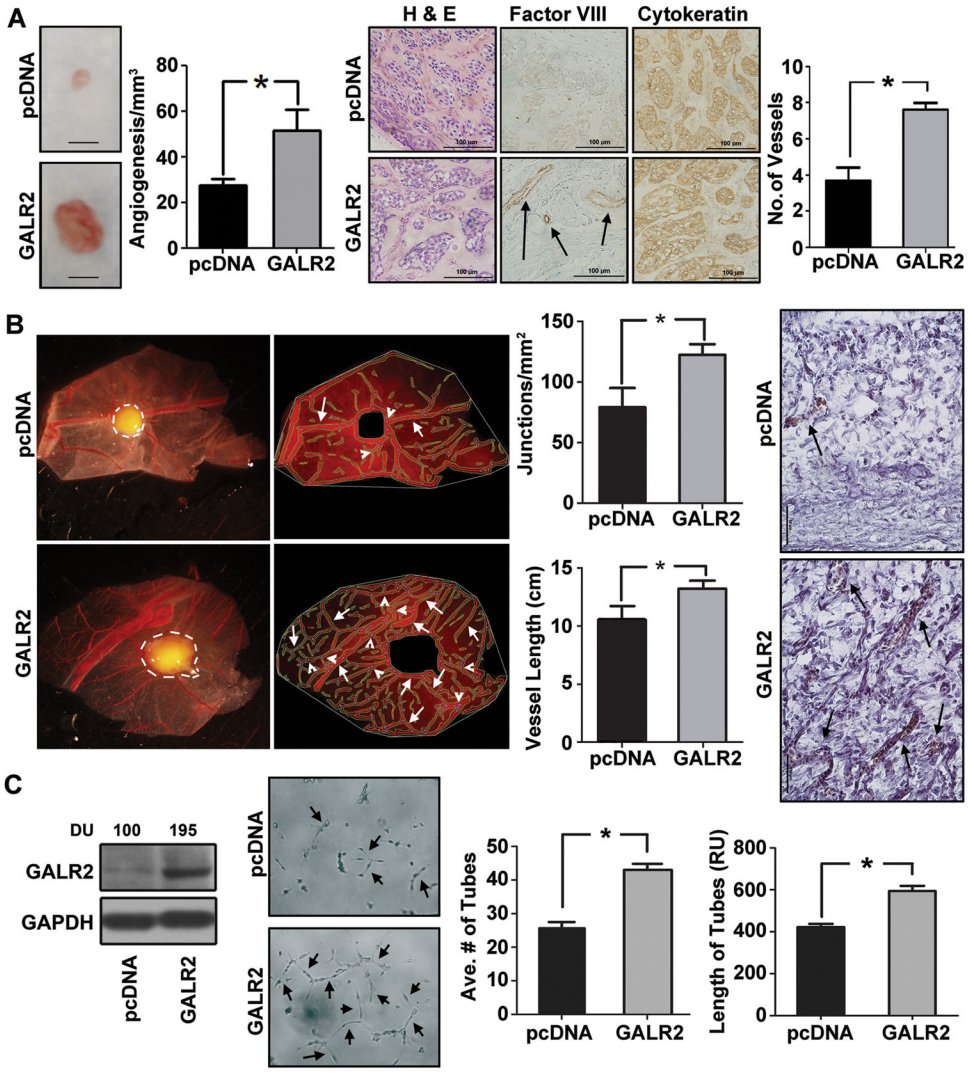

Figure 1. GALR2 induces angiogenesis

(A) Stable mixed clonal population of UM-SCC-1-GALR2 and pcDNA control cells (1 million) were injected subcutaneously in mouse (n=10, 5 in each group) and xenograft tumors were excised. A representative tumor and control is shown (bar=1cm). The neovasculature was quantified and graphed (middle-left panel, *p<0.007). Both control and UM-SCC-1-GALR2 tumor sections were stained with H&E, Factor-VIII and cytokeratin (middle-right panel). Number of vessel from endothelial cells was quantified from each group from five representative fields and graphed (right panel, *p<0.01). **(B)** UM-SCC-1-GALR2 and control cells were placed on the top of the upper CAM (n=10, 5 in each group). After three days, upper CAM was excised and photographed along with the tumor (white border line). Angiogenic structure defined by AngioTool program (white arrowheads, middle-left panel) was calculated for each tumor and total length of tubule normalized to surface area and number of junctions were calculated for each group (middle-right panel, *p<0.012). Histology of the corresponding tumors show vasculature in UM-SCC-1-GALR2 (arrowheads) and control tumors (right panel *p< 0.008). **(C)** UM-SCC-1-GALR2 and

pcDNA cells were immunoblotted with GALR2 and GAPDH antibodies. Band Intensities were quantified by ImageJ software and expressed as arbitrary densitometric unit (DU) normalized to control (left panel). Conditioned media (CM) from UM-SCC-1-GALR2 and pcDNA cells were normalized to equal cell number and incubated overnight on Matrigel seeded with HMEC-1 cells and photographed at 24h (middle-left panel). Both average number of tubes and length of tubes were calculated from 10 representative fields (*$p<0.01$). All experiments were performed three times in triplicate and data shown from one representative experiment.

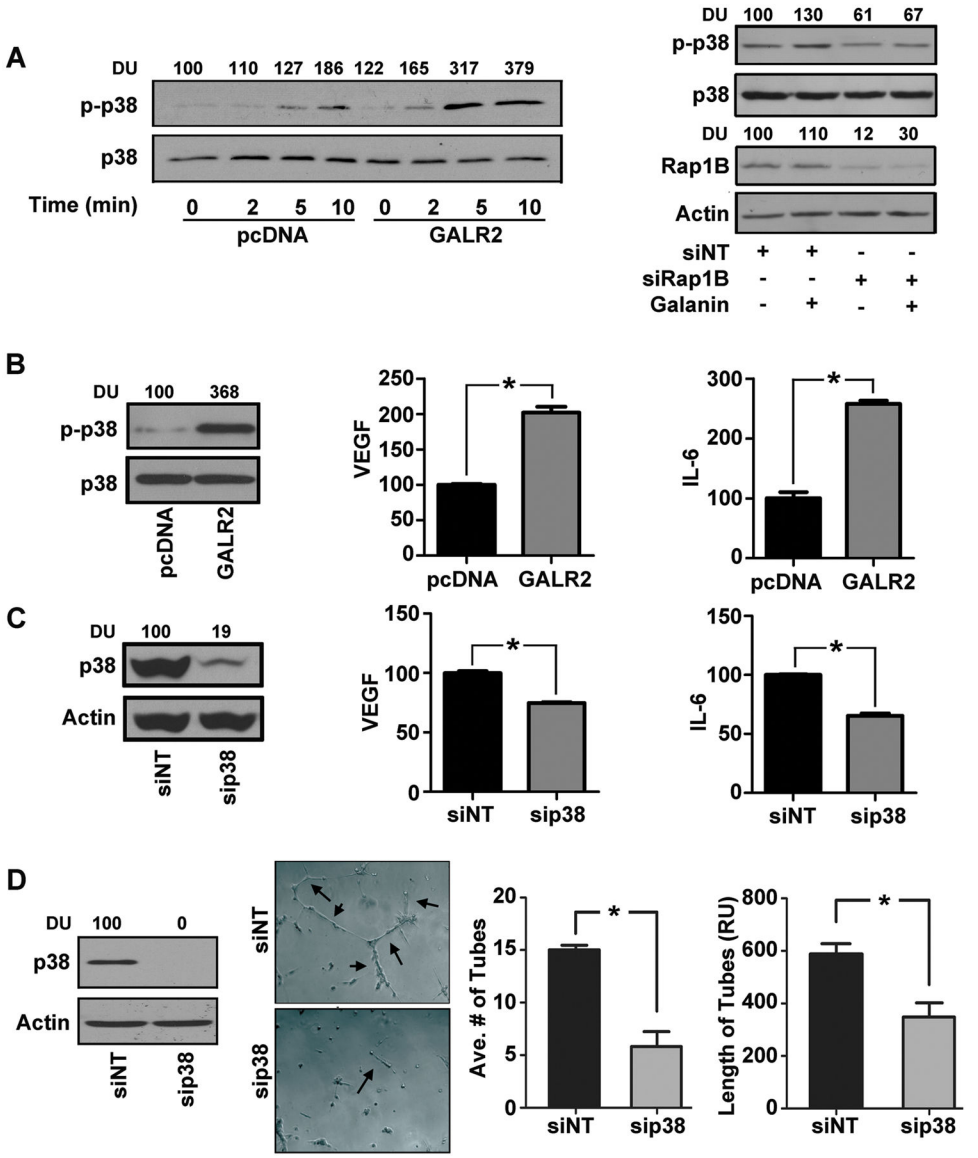

Figure 2. GALR2 stimulates cytokine secretion and angiogenesis via RAP1B-p38-MAPK

(A) Stable mixed clonal population of UM-SCC-1-GALR2 or control pcDNA cells were serum starved for 4h and treated with 10nM Galanin for 0, 2, 5, or 10 minutes. Whole cell lysates were immunoblotted for phospho-p38 and p38 antibodies, quantified (DU) and expressed as percent of control (left panel). UM-SCC-1-GALR2 stable cells were treated with NT-siRNA or si-RAP1B. After 68h of transfection cells were serum starved for 4h and were either stimulated with 10nM galanin or vehicle control for 10 minutes. Both stimulated and unstimulated controls were immunoblotted with actin, RAP1B, p-p38 and p38 antibodies and were quantified (right panel). **(B)** UM-SCC-1-GALR2 or control cells were immunoblotted with p-p38 and total p38 antibodies (left panel). CM were collected and VEGF and IL-6 were quantified with ELISA as pg/ml/million cells and was finally expressed with normalization to control (right panels, *p<0.014). **(C)** UM-SCC-1-GALR2 cells were treated with si-p38 or NT-siRNA and were immunoblotted with p38 and actin

antibodies (left panel). CM collected from cells were quantified for VEGF and IL-6 and expressed as normalized to control (right panel, *p<0.01). **(D)** UM-SCC-1-GALR2 cells were treated with si-p38 or NT-siRNA and immunoblotted (left panel). CM was collected, concentrated, normalized for equal cell count and HMEC-1 cells were seeded with corresponding CM and photographed (middle-left panel). Average number of tubes and tube length were quantified from 10 representative fields (right panel). Data is representative of three identical experiments each in triplicate (*p<0.008).

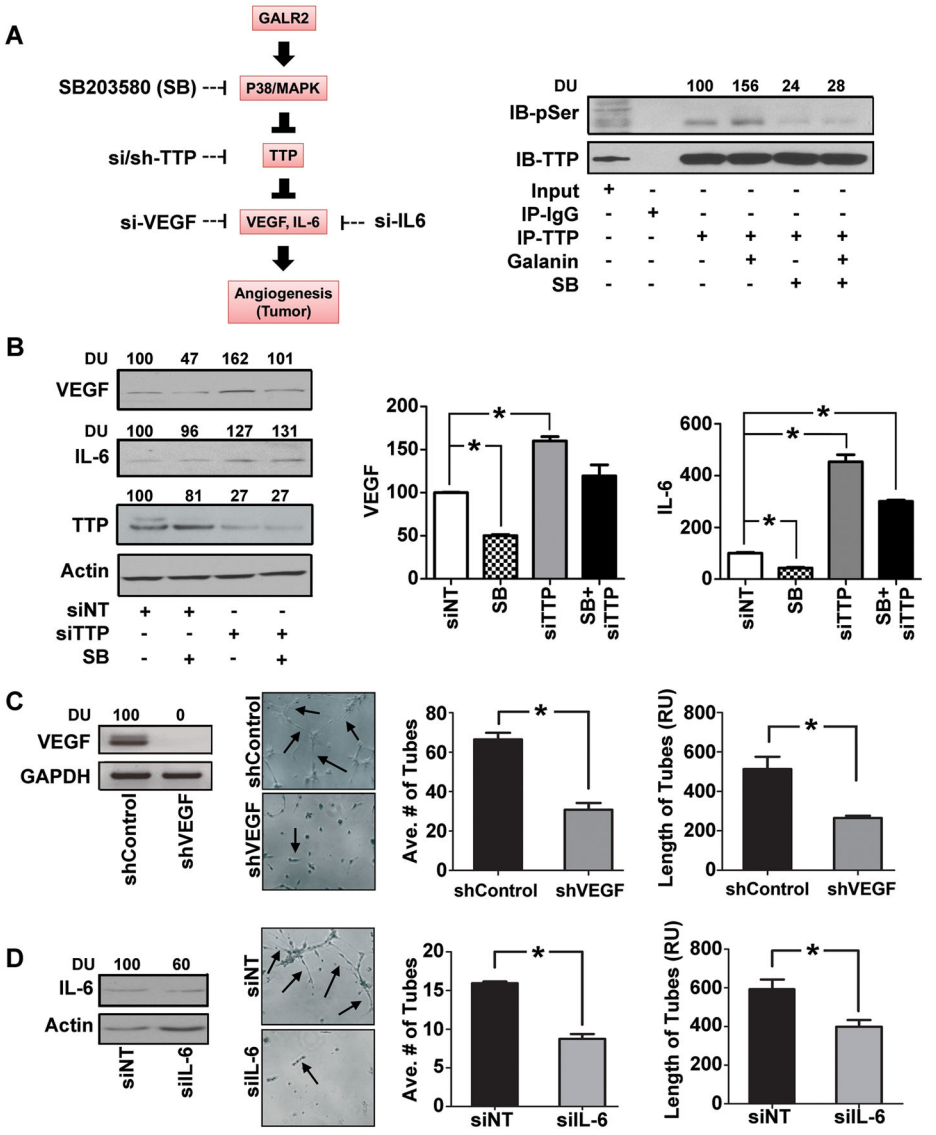

Figure 3. GALR2 induces p38-mediated inhibition of TTP to enhance angiogenesis

(A) Schematic representation of signaling pathway showing GALR2 mediated phosphorylation and activation of p38 that inhibits TTP via phosphorylation. Inactivation or genetic loss (by siRNA) of TTP prevents cytokine degradation giving rise to overall steady state increase in cytokines and acts as angiogenic switch to tumor growth. Chemical inhibitor (SB203580) to p38 kinase activity can dephosphorylate TTP to its active form and degrade cytokines. Alternatively targeting individual cytokines by siRNA could be used to control this angiogenic signal. Upstream inhibitors to angiogenesis might be a better treatment option (left panel). UM-SCC-1-GALR2 cells were serum starved for 4h and then treated with 10μM of SB203580 for 2h and were then stimulated with 10nM galanin for 10 minutes or vehicle control. Clarified cell lysates were immunoprecipitated with TTP antibody, and blotted with anti-TTP and anti-phosphoserine antibodies (right panel). **(B)** UM-SCC-1-GALR2 cells were transfected with siTTP or NT-siRNA and were treated with 10μM of SB203580 or vehicle control. Cell lysates were immunoblotted with VEGF, IL-6,

TTP and actin antibodies (left panel). CM was collected from each of the treatment groups and ELISA was performed for VEGF and IL-6 (right panels) and was quantified as pg/ml/million cells and was finally normalized to control. **(C)** UM-SCC-1-GALR2 cells were transduced with shVEGF and control shRNA lentiviral particles and immunoblotted with VEGF antibody and GAPDH. *In-vitro* tubule formation assay was performed with HMEC-1 cells incubated with corresponding CM collected from cells. Both average and relative number of tubes were quantified from 10 representative fields (*$p<0.02$). **(D)** IL-6 was transiently down regulated in UM-SCC-1-GALR2 cells with si-IL-6 and immunoblotted (left panel) and similarly *in-vitro* tubule formation assay was performed with CM collected from cells (middle-left panel) and quantified (right panel, *$p<0.02$). Data is representative of three identical experiments in triplicate.

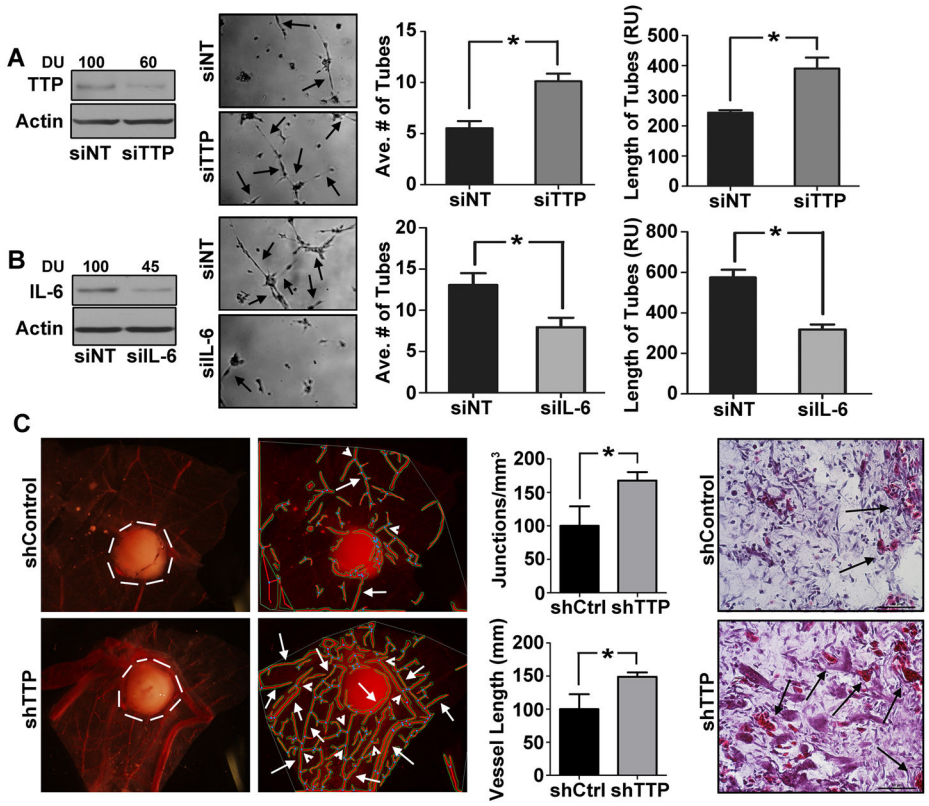

Figure 4. Down regulation of TTP promotes angiogenesis

(A) TTP was transiently downregulated in UM-SCC-1 cells with siTTP or NT and immunoblotted with TTP and actin antibodies (left panel). CM, concentrated and normalized to cell number, was seeded with HMEC-1 cells for *in-vitro* tubule formation assay. Data were quantified from 10 representative fields (middle and right panels respectively,*p<0.003) **(B)** IL-6 was transiently downregulated in UM-SCC-1-shTTP stable cells. Cell lysates were immunoblotted for IL-6 and actin (left panel). CM were collected and *in-vitro* tubule formation assay was performed. Data were quantified from 10 representative fields (middle and right panel respectively (*p<0.05). **(C)** UM-SCC-1-shTTP and control cells (1 million) were dropped on the top of the upper CAM (n=10, 5 for each group). After 36h the CAM was excised and photographed along with the tumor (white border line). Angiogenic structure was determined (white arrowheads, middle-left panel) and calculated as described (middle-right panel, *p<.012 and *p<0.008). Histology of the corresponding tumors show vascularity in UM-SCC-1-shTTP and control tumors (right panel).

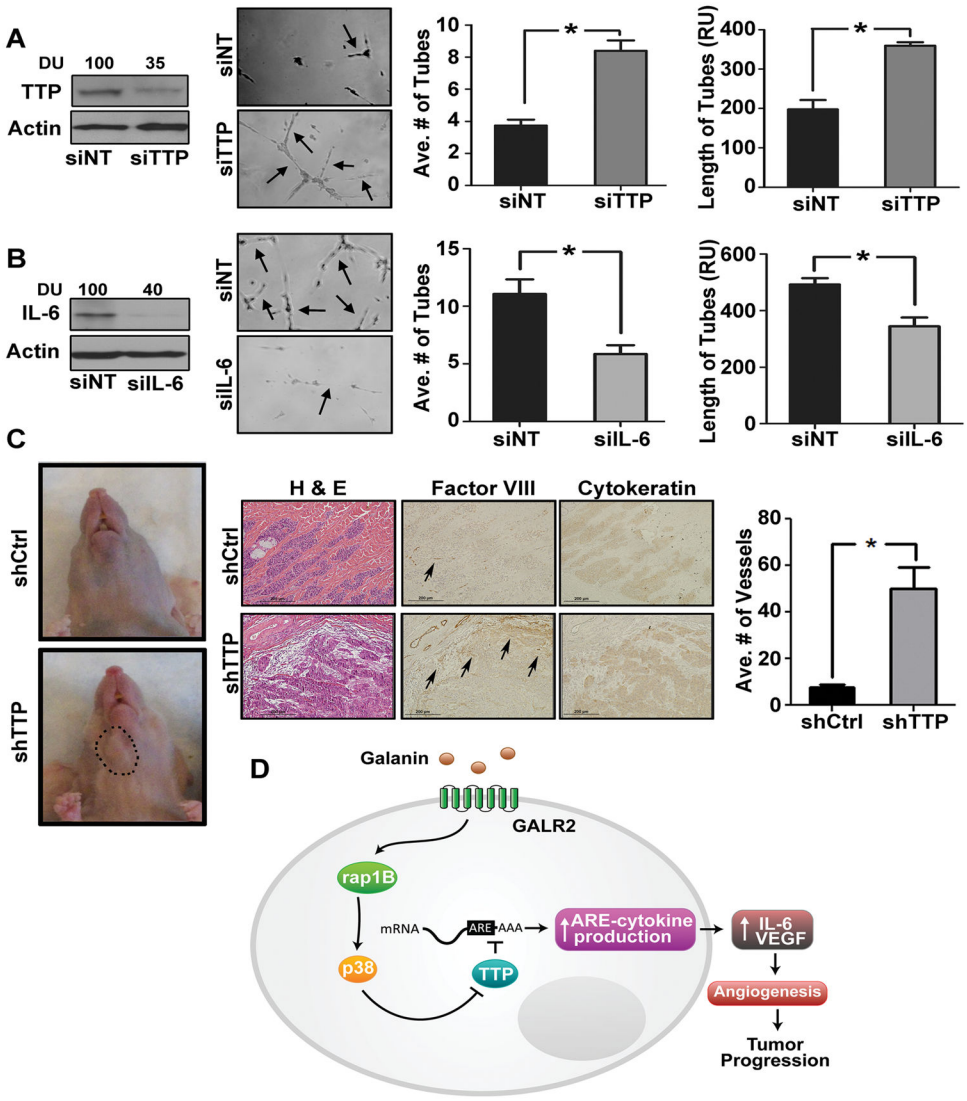

Figure 5. Loss of TTP induce angiogenesis and tumor growth in murine floor-of-mouth

(A) TTP was transiently downregulated in UM-SCC-81B cells, immunoblotted for TTP and actin (left panel). *In-vitro* tubule formation assay was performed with CM collected from these cells (middle-left panel). Average number and length of tubes were quantified from 10 representative fields (right panel *p<0.001). **(B)** IL-6 was transiently downregulated in UM-SCC-81B-shTTP cells. Cell lysates were immunoblotted for IL-6 and actin (left panel). *In-vitro* tubule formation assay was performed and quantified for 10 fields (middle-left and right panel respectively) (*p<0.02). **(C)** UM-SCC-81B-shTTP and shControl (scramble) cells were implanted in the floor-of-mouth of nude mice (n=6). Mice were euthanized when moribund and control mice were euthanized concurrently. A representative image of control and test mice bearing tumor (black circle) is shown (left panel). Sections from the shControl and shTTP tumors were stained with H&E and immunostained with Factor-VIII and cytokeratin antibodies and blood vessels in 10 representative fields were quantified (middle and left panels *p<0.008). **(D)** Summary Figure: Extracellular GAL stimulates GALR2/

RAP1B to induce p38-MAPK to inactivate TTP. Inactivation of TTP inhibits degradation of IL-6 and VEGF mRNA transcripts, thereby causing increased pro-angiogenic cytokine secretion, angiogenesis and tumor growth.